Cotreatment with Vorinostat Enhances Activity of MK-0457 (VX-680) against Acute and Chronic Myelogenous Leukemia Cells

Warren Fiskus,[1] Yongchao Wang,[1] Rajeshree Joshi,[1] Rekha Rao,[1] Yonghua Yang,[1] Jianguang Chen,[1] Ravindra Kolhe,[1] Ramesh Balusu,[1] Kelly Eaton,[1] Pearl Lee,[1] Celalettin Ustun,[1] Anand Jillella,[1] Carolyn A. Buser,[2] Stephen Peiper,[1] and Kapil Bhalla[1]

Abstract

Purpose: We determined the effects of vorinostat (suberoylanalide hydroxamic acid) and/or MK-0457 (VX-680), an Aurora kinase inhibitor on the cultured human (HL-60, OCI-AML3, and K562) and primary acute myelogenous leukemia (AML) and chronic myelogenous leukemia (CML), as well as on the murine pro-B BaF3 cells with ectopic expression of the unmutated and mutant forms of Bcr-Abl.

Experimental Design: Following exposure to MK-0457 and/or vorinostat, apoptosis, loss of viability, as well as activity and levels of Aurora kinase and Bcr-Abl proteins were determined.

Results: Treatment with MK-0457 decreased the phosphorylation of Aurora kinase substrates including serine (S)10 on histone H3 and survivin, and led to aberrant mitosis, DNA endoreduplication as well as apoptosis of the cultured human acute leukemia HL-60, OCI-AML3, and K562 cells. Combined treatment with vorinostat and MK-0457 resulted in greater attenuation of Aurora and Bcr-Abl (in K562) kinase activity and levels as well as synergistically induced apoptosis of OCI-AML3, HL-60, and K562 cells. MK-0457 plus vorinostat also induced synergistic apoptosis of BaF3 cells with ectopic overexpression of wild-type or mutant Bcr-Abl. Finally, cotreatment with MK-0457 and vorinostat induced more loss of viability of primary AML and imatinib-refractory CML than treatment with either agent alone, but exhibited minimal toxicity to normal CD34+ progenitor cells.

Conclusions: Combined *in vitro* treatment with MK-0457 and vorinostat is highly active against cultured and primary leukemia cells. These findings merit *in vivo* testing of the combination against human AML and CML cells, especially against imatinib mesylate–resistant Bcr-AblT315I–expressing CML Cells.

The Aurora kinases are a family of serine/threonine kinases that play an important role in maintaining the fidelity of mitosis by regulating spindle formation, chromosome segregation, and cytokinesis (1–3). Aurora A localizes to the centrosomes and spindle poles and is involved in centrosome maturation and duplication (1–3). Aurora B, a chromosomal passenger protein, localizes to centromeres, midzone microtubules, and midbodies. Aurora B plays a role in chromosomal alignment, spindle assembly checkpoint, and cytokinesis (1–3). The gene encoding Aurora A is on the long arm of chromosome 20 (20q13.2-13.3), a region that is frequently amplified in epithelial cancers (2, 4–6). Aurora A overexpression is also commonly observed in human acute leukemia cells (2). Aurora B is often co-overexpressed with Aurora A (7, 8). Phosphorylation of Aurora A at threonine 288 is required for the kinase activity of Aurora A and for mitotic entry (9, 10). Ectopic overexpression of Aurora A transforms normal cells and leads to aberrant chromosome segregation, genomic instability, and activation of oncogenic pathways (2, 6, 11). Consistent with this, deregulated Aurora kinase activity in cancer cells leads to defects in centrosome function, aberrant spindle assembly, misalignment of chromosomes, abnormal cytokinesis, and genetic instability (6, 11). Several proteins that have important roles in cell division are known substrates phosphorylated by Aurora kinases. These include serine 10 on histone H3, CENP-A, and survivin (12). Due to the pivotal role that Aurora A and Aurora B plays in mitosis, novel agents that abrogate the activities of Aurora A and/or Aurora B kinase have been developed and are being tested for antitumor efficacy (8, 12). MK-0457 (VX-680) is a small molecule inhibitor that inhibits the activity of Aurora A, Aurora B, and Aurora C kinases with inhibition constants (K_i) of 0.6, 18, and 4.6 nmol/L, respectively (1, 12). However, the phenotypic effects induced by treatment with this agent in cancer cells are consistent with Aurora B–specific inhibition similar to AZD1152 and ZM447439 (e.g., depletion of histone H3 serine 10 phosphorylation, inhibition of cell division, misalignment of the chromosomes, and polyploidy; refs. 12, 13). In transformed cells with mitotic checkpoint errors, MK-0457

Authors' Affiliations: [1]Medical College of Georgia Cancer Center, Augusta, Georgia and [2]Merck & Co., Inc., North Wales, Pennsylvania

Received 3/19/08; revised 5/21/08; accepted 5/26/08.

The costs of publication of this article were defrayed in part by the payment of page charges. This article must therefore be hereby marked *advertisement* in accordance with 18 U.S.C. Section 1734 solely to indicate this fact.

Requests for reprints: Kapil Bhalla, MCG Cancer Center, Medical College of Georgia, 1120 15th Street, CN-2101 Augusta, GA 30912. Phone: 706-721-0566; Fax: 706-721-0469; E-mail: kbhalla@mcg.edu.

doi:10.1158/1078-0432.CCR-08-0721

Translational Relevance

This article describes preclinical *in vitro* findings demonstrating the synergistic antileukemia activity of a novel combination of the pan-histone deacetylase inhibitor vorinostat and the Aurora kinase inhibitor MK-0457 in the treatment of acute myelogenous leukemia (AML) and chronic myelogenous leukemia (CML). Treatment with MK-0457 inhibits the activity of Aurora kinase A and B, as well as induces cell cycle G_2-M phase accumulation, endoreduplication, and apoptosis of AML and CML cells. Vorinostat induces acetylation of heat shock protein 90 (hsp90), disrupts the chaperone association of hsp90 with Aurora kinases, thereby depleting Aurora kinase level and activity in AML and CML cells. Importantly, cotreatment with MK-0457 and vorinostat exerts synergistic depletion of Aurora kinases and induces apoptosis of AML and CML cells, including those with imatinib-resistant, dasatinib-resistant, and nilotinib-resistant mutant Bcr-AblT315I. These studies support the rationale for testing the combination of vorinostat and MK-0457 in patients with relapsed AML or CML.

treatment blocks cell cycle progression, leading to accumulation of cells with greater than 4N DNA content, mitotic slippage, ultimately inducing apoptosis (13, 14). At nanomolar concentrations, MK0457 has also been shown to inhibit Fms-related tyrosine kinase-3 (FLT-3) and Bcr-Abl tyrosine kinases, including the imatinib-resistant, nilotinib-resistant, and dasatinib-resistant mutant Bcr-AblT315I (15, 16). Recently, MK0457 showed antileukemia efficacy in patients with imatinib-refractory chronic myelogenous leukemia (CML) harboring Bcr-AblT315I (17).

Vorinostat (suberoylanilide hydroxamic acid) is a hydroxamic acid analogue pan-histone deacetylase inhibitor (HA-HDI; ref. 18). Vorinostat has been shown to inhibit both class I and II HDACs and alter the expression of up to 10% of genes in transformed cells (19). This is associated with growth arrest, differentiation, and apoptosis of human leukemia more than normal cells (19, 20). Treatment with HDIs lead to increased levels of the cell cycle inhibitor proteins p21 and p27, generation of reactive oxygen species, as well as up-regulation of the proapoptotic proteins, e.g., Bax, Bak, and Bim (19–22). HA-HDIs are also known to deplete the levels of antiapoptotic proteins, e.g., Bcl-2, Bcl-x_L, Mcl-1, XIAP, and survivin in human leukemia cells (19–22). By inhibiting HDAC6, a predominantly cytosolic HDAC that is known to deacetylate hsp90 (20–22), treatment with HA-HDIs induces hsp90 acetylation (20, 23). This inhibits the chaperone function of hsp90, which directs hsp90 client proteins, including c-Raf, AKT, FLT-3, and Bcr-Abl, to polyubiquitylation and degradation by the 26S proteasome (23). Thus, treatment with HA-HDIs may not only epigenetically influence gene expression, but through inhibition of hsp90, may also deplete the levels of progrowth and prosurvival proteins, e.g., Bcr-Abl in human leukemia cells. Additionally, our previous findings have highlighted that depletion of the levels of Bcr-Abl with HA-HDI treatment coupled with inhibition of the Bcr-Abl activity by treatment with Bcr-Abl kinase inhibitor imatinib, nilotinib, or dasatinib exerts synergistic apoptotic effects against leukemia cells with wild-type Bcr-Abl (21, 24, 25). Similar effects were noted when mutant FLT-3 was targeted by the combination of HA-HDI with a FLT-3 kinase inhibitor (26). Recent reports indicate that Aurora kinases may also require chaperone association with hsp90, and inhibition of its chaperone function may lead to depletion of Aurora kinases (27). Inhibition of Aurora kinase activity has also been shown to exert anti–acute myelogenous leukemia (AML) activity (13, 28, 29). Taken together, these findings created a strong rationale to determine the antileukemia effects of the combination of vorinostat and MK-0457 against AML and CML cells with unmutated or mutant Bcr-Abl. Findings presented here show that combined treatment with vorinostat and MK-0457 is highly active and exerts superior antileukemia activity than either agent alone against cultured and primary AML and CML cells, including those expressing the P-loop mutant Bcr-AblE255K or the gatekeeper mutation Bcr-AblT315I (25).

Materials and Methods

Reagents and antibodies. MK-0457 and vorinostat were kindly provided by Merck & Co., Inc. Monoclonal c-Abl antibody, and polyclonal anti-STAT5A/B were purchased from Santa Cruz Biotechnology. Monoclonal anti–p-STAT5 and monoclonal antiphosphotyrosine were purchased from BD Biosciences. Polyclonal anti–phospho-Aurora A, anti–phospho-survivin, and monoclonal anti-survivin were purchased from Abcam. Rabbit monoclonal anti–Aurora A, Aurora B, and phospho-Ser10 histone H3 antibodies were purchased from Epitomics, Inc. Antibodies for the immunoblot analyses of p-CrkL and CrkL were purchased from Cell Signaling Technologies. Other reagents and antibodies used in the studies were procured as previously reported (21–26). Mouse monoclonal anti-hsp90, rat monoclonal anti-hsp90, and polyclonal anti-hsp70 antibodies were purchased from StressGen Biotechnologies, Corp. Affinity-purified polyclonal antibody against Ac-K69-hsp90 was generated by Alpha Diagnostic based on the synthetic 12–amino acid peptide flanking K69 (acetylated and unacetylated) ETLTDPSKLDSGK.

Cell lines and cell culture. CML-BC K562 cells and AML HL-60 cells were obtained and maintained in culture, as previously described (23–26). OCI-AML-3 cells were cultured in α-MEM medium with 1% penicillin/streptomycin and 1% nonessential amino acids. Logarithmically growing cells were exposed to the designated concentrations of MK-0457 and/or vorinostat. Following these treatments, cells or cell pellets were washed free of the drug(s) prior to the performance of the studies.

Creation of BaF3/Bcr-Abl, BaF3/Bcr-AblE255K, and BaF3/Bcr-AblT315I cell lines. Mutant p210Bcr-AblE255K and p210Bcr-AblT315I containing plasmids were generated by site-directed mutagenesis, as previously described (21, 25). The p210 Bcr-Abl constructs were nucleofected into BaF3 cells, as previously described (21, 25). After confirmation of Bcr-Abl expression by immunoblot analysis, cells were used for the studies described below.

Primary AML blasts and CML cells. Primary acute myeloid leukemia (AML) and imatinib-resistant CML cells were obtained with informed consent as part of a clinical protocol approved by the Institutional Review Board of the Medical College of Georgia. Peripheral blood or bone marrow aspirate samples were collected in heparinized tubes, and mononuclear cells were separated using Lymphoprep (Axis-Shield), washed once with complete RPMI 1640 medium, resuspended in complete RPMI 1640 and counted to determine the number of cells isolated prior to their use in the various experiments. The purity of the blast populations were confirmed to be 80% or better by morphologic evaluation of cytospun cell preparations stained with Wright stain (24, 25). Banked, de-linked, and de-identified donor peripheral blood

CD34+ mononuclear cells procured for recipients who had since died were purified by immunomagnetic beads conjugated with anti-CD34 antibody prior to use in the cell viability assay (StemCell Technologies).

Cell cycle analysis. Following the designated treatments, cells were harvested and washed twice with 1× PBS and fixed in ethanol overnight. Fixed cells were washed twice with 1× PBS and stained with propidium iodide for 15 min at 37°C. Cell cycle data were collected on a flow cytometer with a 488 nmol/L laser and analyzed with ModFit 3.0, as previously described (24). Cells with <2N DNA content (sub-G_1) were also determined (24).

Confocal microscopy. HL-60, OCI-AML3, and K562 cells were cultured in the presence or absence of MK-0457 for 24 h. Cells were cytospun onto glass slides and fixed with 4% paraformaldehyde for 10 min. Following this, the slides were blocked with 5% bovine serum albumin for 30 min and incubated with FITC-conjugated α-tubulin and Dy547-conjugated γ-tubulin (Abcam) at a dilution of 1:50 in blocking buffer for 2 h. For MPM-2 staining, cells were stained for 1 h with a FITC-conjugated MPM-2 antibody at a 1:100 dilution. Following three washes with PBS, the cells were mounted using Vectashield with 4′,6-diamidino-2-phenylindole and imaged at 63× using a Zeiss LSM510 confocal microscope.

Assessment of apoptosis by Annexin V staining. Untreated or drug-treated cells were stained with Annexin V (Pharmingen) and propidium iodide and the percentage of apoptotic cells were determined by flow cytometry. To analyze the synergism between MK-0457 and vorinostat in inducing apoptosis, cells were treated with MK-0457 (20-150 nmol/L) and vorinostat (0.2-1.5 μmol/L) at a constant ratio of 1:10 for 48 h. The percentage of apoptotic cells was determined by flow cytometry, as previously described (21, 22). The combination index (CI) for each drug combination was obtained by median dose-effect of Chou and Talalay (30) using the CI equation within the commercially available software Calcusyn (Biosoft). CI < 1.0 represents the synergism of the two drugs in combination.

Assessment of percentage of nonviable cells. Following designated treatments, cells were stained with trypan blue (Sigma). The number of nonviable cells were determined by counting the cells that showed trypan blue uptake in a hemocytometer, and was reported as a percentage of untreated control cells.

Cell lysis and protein quantitation. Untreated or drug-treated cells were centrifuged and the cell pellets were resuspended in 200 μL of lysis buffer [20 mmol/L Tris (pH 8), 150 nmol/L sodium chloride 1% Triton X-100, 1 mmol/L phenylmethylsulfonyl fluoride, 10 μg/mL leupeptin, 1 μg/mL pepstatin-A, 2 μg/mL aprotinin, 20 mmol/L p-nitrophenyl phosphate, 1.0 mmol/L sodium orthovanadate, and 1 mmol/L 4-(2-aminoethyl) benzenesulfonylfluoride hydrochloride] and incubated on ice for 30 min. The cell lysates were centrifuged and an aliquot of each cell lysate was diluted 1:10 and protein quantitated using a bicinchoninic acid protein quantitation kit (Pierce), according to the manufacturer's protocol.

Immunoprecipitation of hsp90 and immunoblot analyses. Following the designated treatments, cells were lysed for 30 min on ice, and the nuclear and cellular debris were cleared by centrifugation. Cell lysates (500 μg) were incubated with a rat monoclonal anti-hsp90 antibody (StressGen), for 1 h at 4°C. Washed Protein G agarose beads were added to this solution and incubated overnight at 4°C. The immunoprecipitates were washed thrice in the lysis buffer and proteins were eluted with the SDS sample loading buffer prior to the immunoblot analyses with specific antibodies against acetyl-K69 hsp90, Aurora A, or total hsp90 levels.

SDS-PAGE and Western blotting. One hundred micrograms of total cell lysate was used for SDS-PAGE. Western blot analyses of Bcr-Abl, p-STAT5, pCrkL, p-Aurora A/B, Aurora A, Aurora B, p-survivin, survivin, p-Ser10 histone H3, histone H3, and Bim were done on total cell lysates using specific antisera or monoclonal antibodies. The expression level of either β-actin or α-tubulin was used as the loading control for the Western blots. Blots were developed with a chemiluminescent substrate ECL (Amersham Biosciences).

Statistical analysis. Significant differences between values obtained in a population of leukemic cells treated with different experimental conditions were determined using Student's t test. $P < 0.05$ values were considered significant.

Results

MK-0457 treatment induces cell cycle arrest, multipolar spindle formation, as well as attenuates Aurora kinase activity and induces apoptosis and endoreduplication in cultured CML-BC and AML cell lines. We first determined the effects of MK-0457 treatment on the cell cycle status of the cultured CML-BC K562 and the AML HL-60 and OCI-AML3 cells. Table 1 shows that exposure to increasing concentrations of MK-0457 caused a dose-dependent accumulation of cells in the G_2-M phase with a concomitant decline in the G_1 and S phases of the cell cycle in all of the three cell lines examined. Following a 24-hour exposure to 50 nmol/L of MK-0457, >80% of cells were in the G_2-M phase of the cell cycle in K562 and HL-60 cells. OCI-AML3 cells were relatively less sensitive to the cell cycle effects of MK-0457. Although the greatest cell cycle–inhibitory effects were observed at 24 hours for all three cell lines, treatment with MK-0457 for 8 hours, but not for shorter exposure intervals, resulted in an increase in the percentage of cells in G_2-M (data not shown). Immunofluorescent staining of α-tubulin and γ-tubulin in HL-60 and OCI-AML3 cells, followed by confocal immunofluorescent microscopy, showed that α-tubulin and γ-tubulin localized to the mitotic spindle and the centrosomes, respectively (Fig. 1A). Exposure to MK-0457 for 24 hours resulted in the development of aberrant mitosis showing multiple spindle poles. In HL-60 cells, this was seen after exposure to MK-0457 levels as low as 20 nmol/L, whereas concentrations of ≥50 nmol/L were required to induce multipolar spindles in OCI-AML3 (Fig. 1A) and K562 (data not shown) cells. Also, exposure to MK-0457 dose-dependently decreased the staining of OCI-AML3 cell with a monoclonal

Table 1. MK-0457 treatment induces G_2-M arrest in leukemia cells

Cells and treatment	Cells (%)		
	G_0-G_1	S	G_2-M
K562			
Untreated	26.8 ± 0.6	58.5 ± 2.9	14.7 ± 2.3
20 nmol/L MK-0457	31.6 ± 1.9	0.5 ± 0.2	67.9 ± 1.8
50 nmol/L MK-0457	12.7 ± 3.3	1.5 ± 0.4	85.8 ± 2.9
100 nmol/L MK-0457	3.4 ± 1.5	1.9 ± 0.9	94.7 ± 2.5
HL-60			
Untreated	41.7 ± 1.2	44.3 ± 0.5	14.0 ± 0.8
20 nmol/L MK-0457	36.3 ± 0.8	23.6 ± 0.4	40.1 ± 0.8
50 nmol/L MK-0457	2.3 ± 0.5	17.2 ± 0.9	80.4 ± 0.5
100 nmol/L MK-0457	2.6 ± 0.3	18.5 ± 1.1	78.8 ± 0.9
OCI-AML3			
Untreated	61.6 ± 0.7	30.6 ± 0.5	7.7 ± 0.3
20 nmol/L MK-0457	61.5 ± 0.7	21.8 ± 0.3	16.7 ± 0.4
50 nmol/L MK-0457	37.5 ± 0.9	17.6 ± 0.8	44.9 ± 0.8
100 nmol/L MK-0457	19.9 ± 0.6	16.3 ± 2.5	63.7 ± 0.3

NOTE: K562, HL-60, and OCI-AML3 cells were treated with the indicated doses of MK-0457 for 24 h. Then, the cells were fixed and stained for cell cycle analysis by flow cytometry. Values represent the mean of three experiments ± SE.

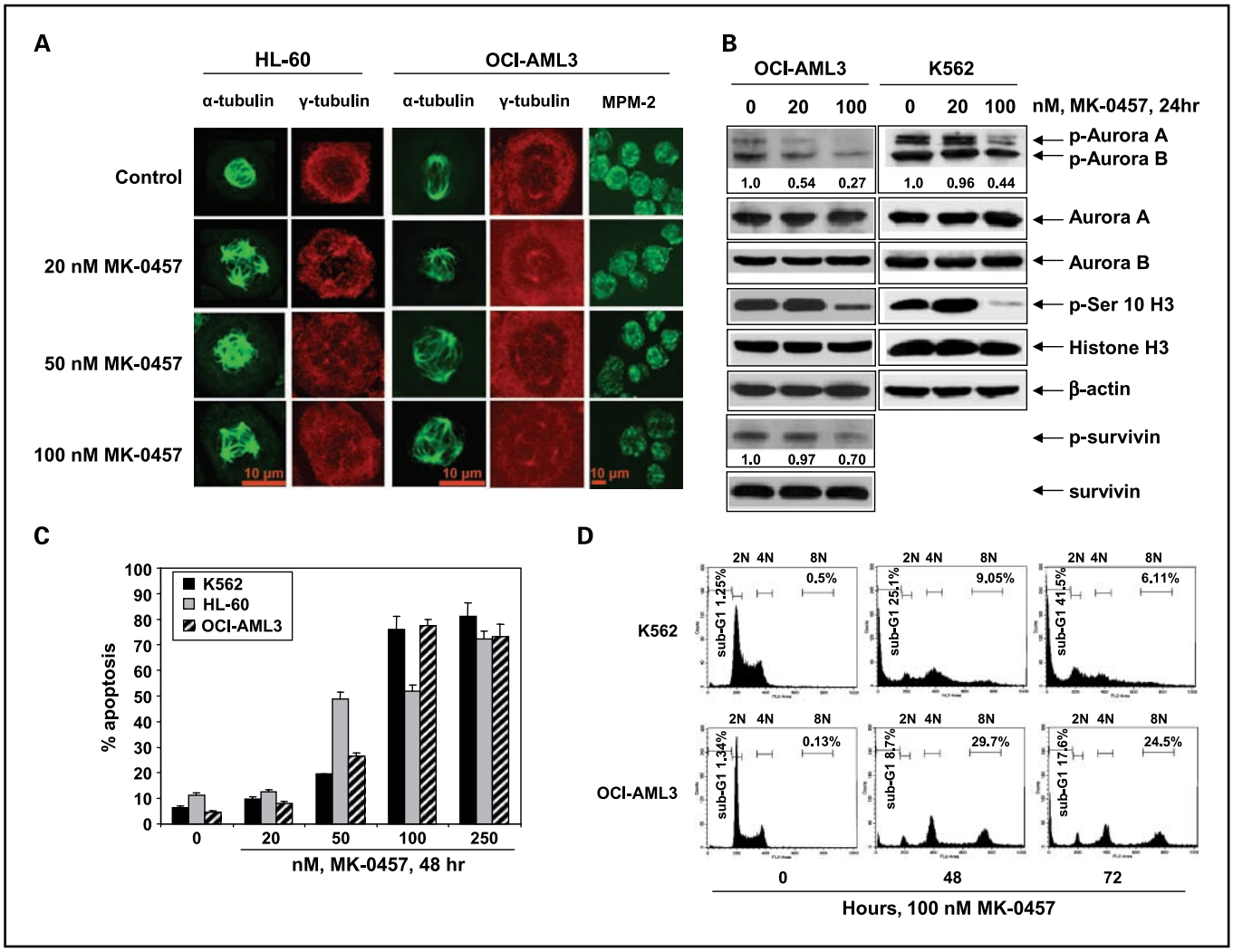

Fig. 1. MK-0457 treatment induces multipolar spindle formation and endoreduplication in acute leukemia cells. *A,* HL-60 and OCI-AML3 cells were treated with the indicated doses of MK-0457 for 24 h. Following this, cells were fixed with paraformaldehyde and stained with anti–α-tubulin, anti–γ-tubulin, or anti–MPM-2 antibodies and imaged at 63× by confocal microscopy. *B,* OCI-AML3 (*left*) and K562 (*right*) cells were treated with the indicated doses of MK-457 for 24 h. Following this, immunoblot analysis was done on total cell lysates or extracted histones for p-Aurora A/B, Aurora A, Aurora B, p-survivin, survivin, and p-Ser10 histone. The levels of β-actin or total histone H3 in the cell lysates served as the loading control. *C,* K562, HL-60, and OCI-AML3 cells were treated with the indicated doses of MK-0457 for 48 h. Following treatment, the percentages of Annexin V–stained apoptotic cells were determined by flow cytometry. Columns, mean of three experiments; bars, SE. *D,* K562 and OCI-AML3 cells were treated with 100 nmol/L of MK-0457 for the indicated times. Then, the cells were fixed and stained with propidium iodide and DNA content was determined by flow cytometry.

MPM-2 antibody (which stains mitotic phosphoproteins), as shown by immunofluorescent microscopy (Fig. 1A). K562 and HL-60 cells do not contain increased copy numbers (gene amplification) of the Aurora A gene, as determined by fluorescence *in situ* hybridization, using a probe containing the entire Aurora A gene and an additional 71-kb of the downstream sequence of the long arm of chromosome 20 (data not shown). We next determined the inhibitory effects of MK-0457 on Aurora kinase and MK-0457–induced apoptosis in the cultured acute leukemia OCI-AML3, HL-60, and K562 cells. Figure 1B shows that exposure of OCI-AML3 cells to MK-0457 (20 or 100 nmol/L) depleted the kinase activity of Aurora A and Aurora B, as measured by the decrease in levels of autophosphorylated Aurora A and Aurora B, without affecting the levels of Aurora A and Aurora B. Exposure to 100 nmol/L of MK-0457 was also accompanied by decreased levels of the phosphorylated serine 10 on histone H3 (Fig. 1B). Treatment with MK-0457 exerted similar effects in K562 cells (Fig. 1B). MK-0457 also depleted the levels of threonine 34–phosphorylated survivin in OCI-AML3 and K562 cells (see below), without affecting survivin levels (Fig. 1B). Exposure to 20 to 250 nmol/L of MK-0457 dose-dependently induced apoptosis of K562, HL-60, and OCI-AML3 cells (Fig. 1C). Following exposure to 100 nmol/L of MK-0457, >75% of K562 and OCI-AML3 cells were apoptotic, whereas apoptosis of 55% of HL-60 cells was observed (Fig. 1C). We next determined whether MK-0457 induced endoreduplication of DNA in the leukemia cells. Treatment of K562 and OCI-AML3 cells with 100 nmol/L of MK-0457 for 48 hours led to an increase in the percentage of cells with 8N DNA content (Fig. 1D). Endoreduplication was most evident in OCI-AML3 cells, with nearly 30% of cells possessing greater than 4N DNA content compared with 9.0%

in K562 cells. After 72 hours of exposure, the percentage of cells with 8N DNA content decreased in both OCI-AML3 and K562 cells (Fig. 1D). This was due to the increase in the percentage of cells with <2N DNA (sub-G_1) content to 17.6% and 41.5%, respectively. Taken together with the observed decrease in MPM-2 staining and increased endoreduplication, this suggested "mitotic slippage" and increased apoptosis.

Vorinostat depletes Aurora A kinase levels and enhances MK-0457–mediated apoptosis in AML and CML-BC cells. In previous reports, we showed that treatment with vorinostat induces the levels of the prodeath proteins and depletes prosurvival proteins, which is associated with growth arrest and apoptosis of acute leukemia cells (23, 25). We have also previously shown that HDAC inhibitors disrupt the chaperone association of hsp90 with its client proteins (23). We next determined the effects of vorinostat treatment on the chaperone association of hsp90 with Aurora A in OCI-AML3 cells. Treatment with vorinostat for 8 hours resulted in an abrogation of the binding of Aurora A with hsp90 in hsp90 immunoprecipitates, as well as an increase in acetylated hsp90 as determined by immunoblot analysis following staining with an acetylated lysine 69-specific hsp90 antibody. We also observed depletion of the levels of Aurora A in total cell lysates as well as induction of hsp70 and total cellular levels of acetylated hsp90 (Fig. 2A). We next determined whether vorinostat-mediated depletion of Aurora A and Aurora B was due to their proteasomal degradation. Figure 2B shows that partial depletion of Aurora A, Aurora B, and c-Raf due to treatment of OCI-AML3 cells by vorinostat was restored by cotreatment with the proteasome inhibitor bortezomib. Here, the levels of c-Raf, which is chaperoned by hsp90, served as the positive control (21). Similar effects were observed in K562 cells following treatment with vorinostat and bortezomib (data not shown). These data suggest that vorinostat-mediated depletion of Aurora A and Aurora B is at least partially due to the disruption of chaperone association of hsp90 with Aurora A and B, leading to their degradation by the 26S proteasome. We next determined the effects of vorinostat and/or MK-0457 on the levels and activity of Aurora kinases in the cultured acute leukemia HL-60, OCI-AML3, and K562 cells. Figure 2C shows that treatment with 1.0 μmol/L of vorinostat alone attenuated the total Aurora A and B levels in OCI-AML3 and K562 cells.

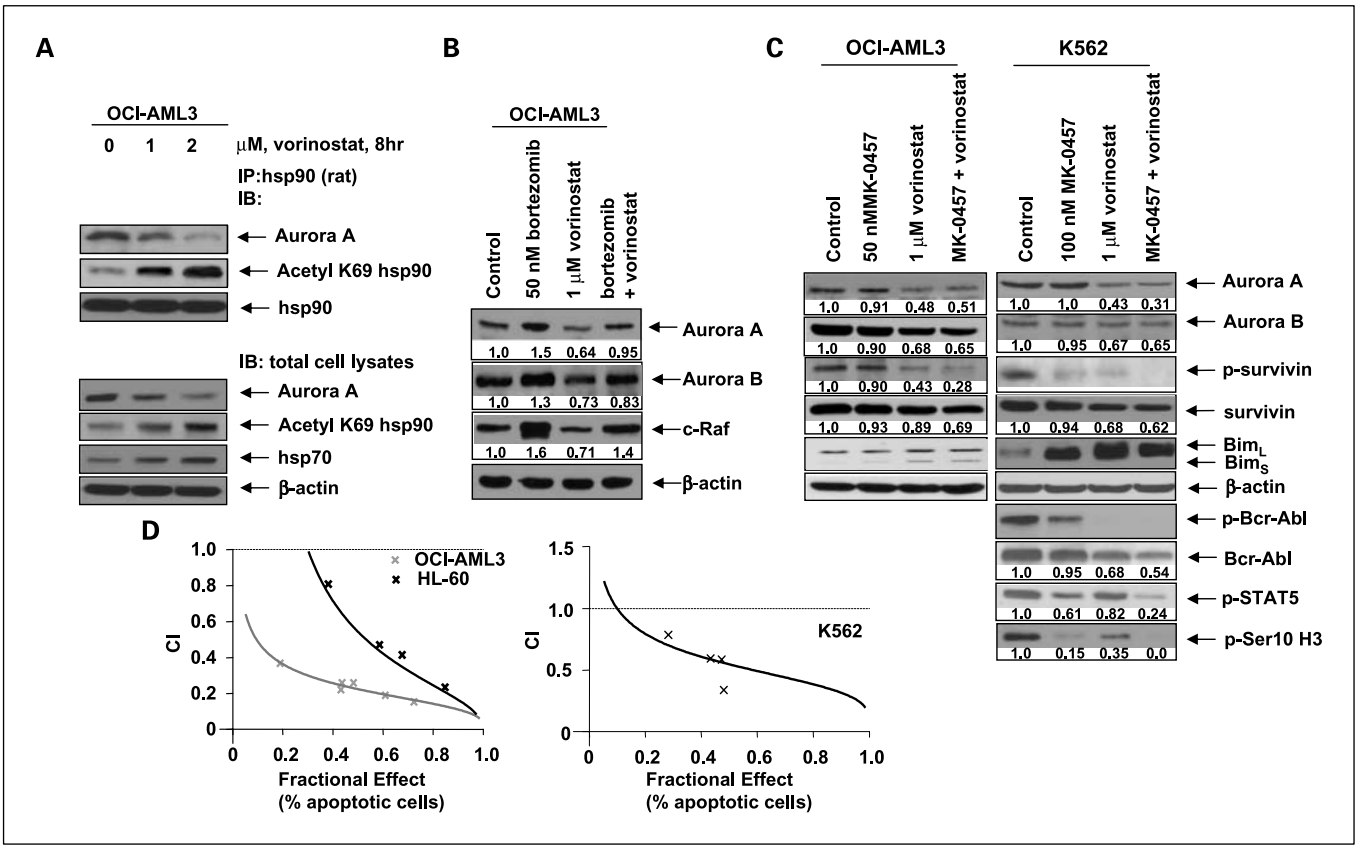

Fig. 2. Vorinostat depletes the levels of Aurora A, inhibits its chaperone association with hsp90, induces Bim expression, and combined treatment with MK-0457 exerts synergistic apoptotic effects in AML cells. *A,* OCI-AML3 cells were treated with vorinostat for 8 h. Following this, hsp90 was immunoprecipitated from the cell lysates and immunoblot analysis was done for Aurora A, acetylated K69 hsp90, and total hsp90 levels. Alternatively, immunoblot analysis was done for Aurora A, hsp70, and acetylated K69 hsp90. The levels of β-actin in the cell lysates served as the loading control. *B,* OCI-AML3 cells were treated with the indicated doses of bortezomib and/or vorinostat for 16 h. Immunoblot analysis was done for Aurora A, Aurora B, and c-Raf on the total cell lysates. The levels of β-actin in the lysates served as the loading control. Densitometry was done with ImageQuant version 5.2. *C,* OCI-AML3 and K562 cells were treated with the indicated doses of MK-0457 and/or vorinostat for 24 h. Western blot analysis was done for p-Aurora A/B, Aurora A, Aurora B, p-survivin, total survivin, and Bim on the total cell lysates. Additionally, immunoblot analysis was done for p-Bcr-Abl, Bcr-Abl, p-STAT5, and p-Ser10 H3 in K562 cells. The levels of β-actin in the cell lysates served as the loading control. *D,* analysis of dose-effect relationship for MK-0457 (20-150 nmol/L) and vorinostat (0.2-2.0 μmol/L) for the apoptotic effects after 48 h of exposure in HL-60, OCI-AML3 (*left*), and K562 (*right*) cells was done according to the median dose-effect method of Chou and Talalay. Following this, the CI values were calculated. CI < 1, CI = 1, and CI > 1 represent synergism, additivity, and antagonism of the two agents, respectively.

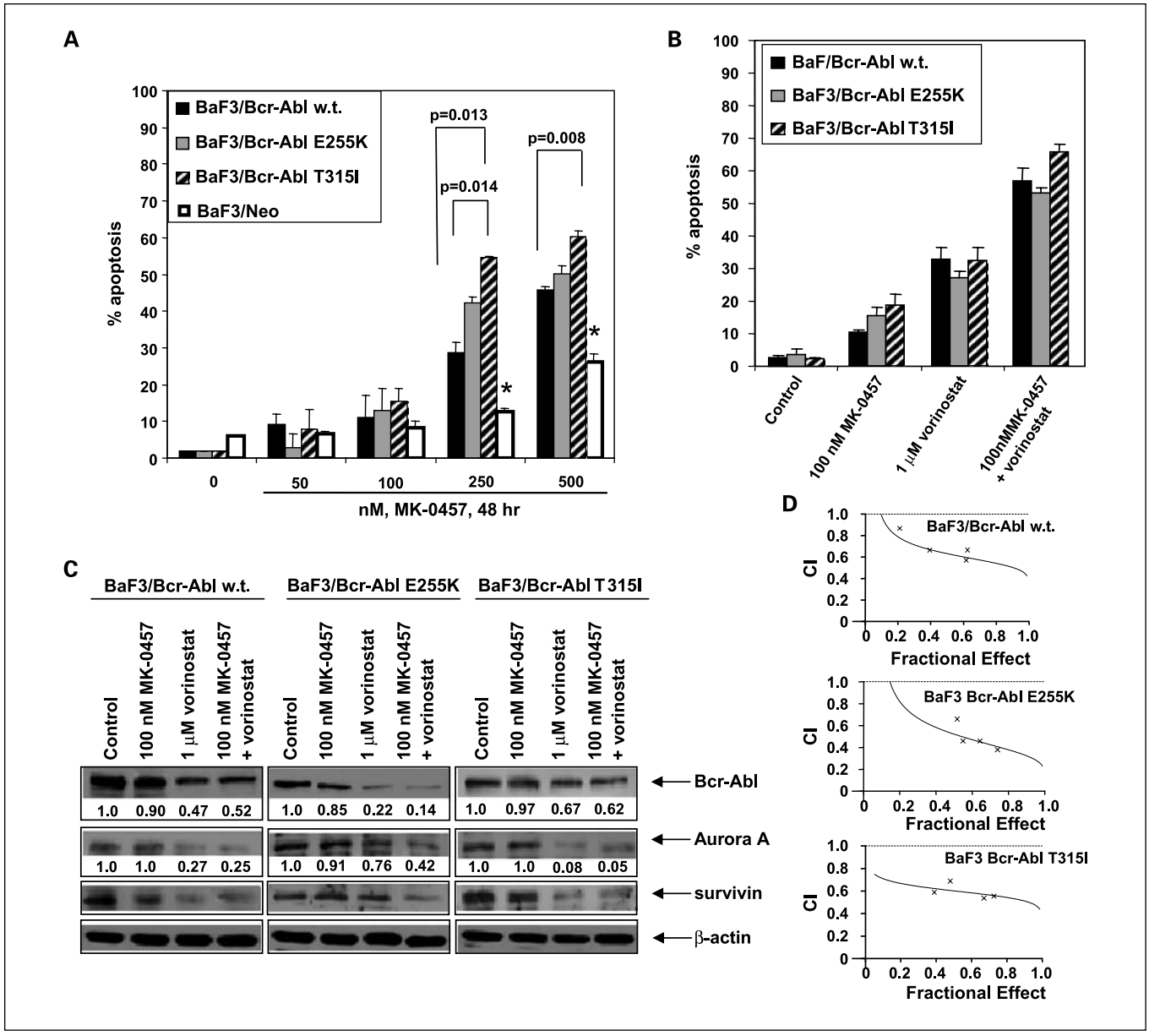

Fig. 3. Effects of MK-457 and/or vorinostat on BaF3 cells expressing unmutated and mutant forms of Bcr-Abl. *A,* BaF3/Bcr-Abl wild-type, BaF3/Bcr-AblE255K, BaF3/Bcr-AblT315I cells, and BaF3/Neo cells were treated with the indicated concentrations of MK-0457 for 48 h. Then the percentages of Annexin V – positive apoptotic cells were assessed by flow cytometry. Columns, mean of three experiments; bars, SE. The *P* values indicate the level of statistical significance of the two values compared; *, significantly less value as compared with similarly treated BaF3/Bcr-Abl wild-type, BaF3/Bcr-AblE255K, and BaF3/Bcr-AblT315I cells. *B,* BaF3/Bcr-Abl wild-type, BaF3/Bcr-AblE255K, and BaF3/Bcr-AblT315I cells were treated with the indicated concentrations of MK-0457 and/or vorinostat for 48 h. Following this, the percentage of Annexin V – positive apoptotic cells was determined by flow cytometry. Columns, mean of three experiments; bars, SE. *C,* BaF3/Bcr-Abl wild-type, BaF3/Bcr-AblE255K, and BaF3/Bcr-AblT315I cells were treated with the indicated concentrations of MK-0457 and/or vorinostat for 24 h. Immunoblot analysis was done for Bcr-Abl, Aurora A, and survivin. The level of β-actin in the lysates served as the loading control. *D,* analysis of dose-effect relationship for MK-0457 (50-150 nmol/L) and vorinostat (0.2-1.5 μmol/L) for the apoptotic effects after 48 h of exposure in BaF3/Bcr-Abl wild-type, BaF3/Bcr-Abl E255K, and BaF3/Bcr-Abl T315I cells was done according to the median dose-effect method of Chou and Talalay. Following this, the CI values were calculated for each cell line.

Although vorinostat only slightly depleted the total survivin levels, it attenuated p-survivin levels. Conversely, treatment with vorinostat alone increased the levels of the long and short isoforms of Bim (Bim_L and Bim_S) in OCI-AML3 cells (Fig. 2C). Notably, cotreatment with vorinostat (1.0 μmol/L) and MK-0457 (50 nmol/L) caused greater depletion of p-survivin in OCI-AML3 cells than treatment with either agent alone (Fig. 2C, *left*). Combined treatment also induced slightly more Bim_L and Bim_S expressions in OCI-AML3 cells. Vorinostat and/or MK-0457 exerted similar effects in HL-60 cells (data not shown). In K562 cells, combined treatment with vorinostat (1.0 μmol/L) and MK-0457 (100 nmol/L) caused more depletion of p-survivin, survivin, and Aurora A levels, whereas Bim induction was slightly less than what was observed following treatment with vorinostat alone (Fig. 2C). However, cotreatment with vorinostat and MK-0457 caused more depletion of p-STAT5, as well as of Bcr-Abl than treatment with either agent alone. This was also associated with a

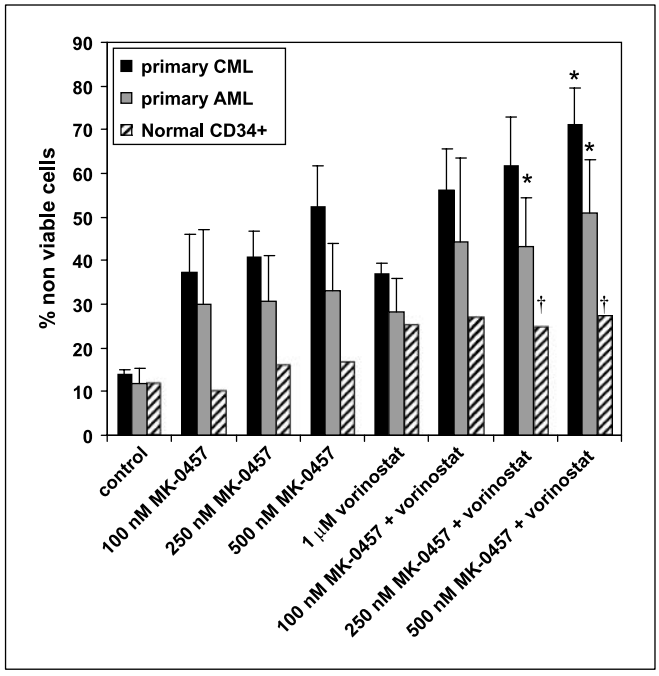

Fig. 4. Vorinostat enhances MK-0457–mediated loss of viability of primary AML and CML cells. Bone marrow samples from four CML, three AML patients, and two normal CD34+ samples were treated with the indicated concentrations of MK-0457 and/or vorinostat for 48 h. Following this, the percentages of nonviable cells for each drug alone or in combination were determined by trypan blue dye uptake in a hemocytometer. Columns, mean; bars, SE. *, $P < 0.05$, significantly greater values than those following treatment with either agent alone at the indicated concentrations in the CML and AML samples. †, $P < 0.05$, significantly lower values in normal CD34+ versus leukemia samples for the drug combinations.

profound attenuation of p-Bcr-Abl and phosphorylated serine 10 on histone H3, p-survivin and Aurora A expression. We next determined the apoptotic effects of cotreatment with MK-0457 and vorinostat. As compared with treatment with either agent alone, cotreatment with vorinostat and MK-0457 synergistically induced apoptosis of OCI-AML3, HL-60, and K562 cells, as determined by the median dose-effect method described by Chou and Talalay (Fig. 2D, *left* and *right*). For MK-0457 and vorinostat, the CI values were <1.0 for all the tested doses of the two drugs.

MK-0457 inhibits activity of Bcr-Abl and induces cell death in BaF3 cells with overexpression of unmutated or mutant Bcr-Abl. We next determined the activity of MK-0457 against murine pro-B BaF3 cells with ectopic overexpression of either wild-type (unmutated) Bcr-Abl or the point mutants Bcr-Abl E255K and Bcr-Abl T315I. Treatment with MK-0457 (100-500 nmol/L) dose-dependently increased the percentage of apoptotic cells in BaF3 with wild-type or mutant forms of Bcr-Abl (Fig. 3A). Higher concentrations of MK-0457 induced significantly more apoptosis of the BaF3/Bcr-AblT315I and BaF3/Bcr-AblE255K versus BaF3/Bcr-Abl cells (Fig. 3A), whereas the control BaF3/Neo cells were the least sensitive to MK-0457 ($P < 0.01$; Fig. 3A). These data also show that MK-0457 is highly active against Bcr-AblT315I–expressing cells, which are otherwise quite resistant to imatinib, dasatinib, and nilotinib (21, 24, 25). Less activity against BaF3/Neo cells also suggests that the ectopic expression of the wild-type or mutant forms of Bcr-Abl makes BaF3 cells more sensitive to MK-0457, and that most of the lethal effects of MK-0457 are dependent on its anti–Bcr-Abl activity in Bcr-Abl–expressing BaF3 cells. Cotreatment with vorinostat (1.0 μmol/L) and MK-0457 (100 nmol/L) also induced significantly more loss of cell viability in BaF3 cells with wild-type or mutant forms of Bcr-Abl, as compared with treatment with either agent alone ($P < 0.01$; Fig. 3B). This was associated with considerable depletion of Bcr-Abl, Aurora A, and survivin levels in BaF3 cells expressing either the wild-type or mutant forms of Bcr-Abl, following cotreatment with vorinostat and MK-0457 (Fig. 3C). Importantly, the median dose-effect method showed that combined treatment with vorinostat (0.5-2 μmol/L) and MK-0457 (50-200 nmol/L) exerted synergistic apoptotic effects against BaF3/Bcr-AblT315I, Bcr-AblE255K, and BaF3/Bcr-Abl cells (Fig. 3D). For MK-0457 and vorinostat, the CI values were <1.0 for all of the tested doses of the two drugs.

Cotreatment with MK-0457 and vorinostat inhibits Aurora kinase activity and exerts superior antileukemia activity against primary CML and AML cells. We next determined the antileukemia effects of MK-0457 and/or vorinostat against four imatinib-refractory primary CML cells, three AML blast samples, as well as against normal human CD34+ progenitor cells. For the CML samples, the mechanism underlying imatinib refractoriness was unknown. Figure 4 shows that treatment with MK-0457 (100-500 nmol/L) or 1.0 μmol/L of vorinostat induced loss of cell viability of the primary CML and AML cells to a variable extent. However, as compared with treatment with either agent alone, cotreatment with MK-0457 and vorinostat induced more loss of cell viability in each of the CML and AML samples tested. When mean values for the loss of cell viability in CML and AML samples were considered, the combination of 500 nmol/L of MK-0457 and vorinostat (1.0 μmol/L) induced more loss of cell viability than either agent alone (Fig. 4). Notably, normal CD34+ progenitor cells were, in general, less susceptible to the toxic effect of MK-0457 than AML or CML cells (Fig. 4). Additionally, cotreatment with MK-0457 (100-500 nmol/L) and vorinostat (1.0 μmol/L) induced more loss of cell viability in CML or AML versus normal CD34+ progenitor cells. One AML and one CML sample yielded a sufficient number of cells to allow for immunoblot analysis of Aurora kinase activity and levels. Similar to the cultured OCI-AML3 and K562 cells, treatment with MK-0457 alone inhibited p-Aurora A, p-Aurora B, and p-survivin levels in the primary AML and CML cells (Fig. 5A). In the primary CML cells, MK-0457 also induced Bim_{EL} levels in a dose-dependent manner. In primary CML and AML cells, cotreatment with MK-0457 (50 nmol/L) and vorinostat (1.0 μmol/L) attenuated p-Aurora A, p-Aurora B, and p-survivin levels, as well as induced Bim_{EL} to a greater extent than treatment with either agent alone (Fig. 5B-C). As was observed in K562 cells, in primary CML cells, cotreatment with MK-0457 (100 nmol/L) and vorinostat (1.0 μmol/L) also caused greater depletion of Bcr-Abl, p-STAT5, and p-CrkL than treatment with either agent alone (Fig. 5D). These findings are consistent with the greater loss of cell viability observed in primary AML and CML cells, following cotreatment with vorinostat and MK-0457 (Fig. 4).

Discussion

Although individually, both vorinostat and MK-0457 have been reported to induce *in vitro* growth arrest and apoptosis of

human AML cells (13, 18), in the present studies, we show for the first time that combined treatment with vorinostat and MK-0457 synergistically induces apoptosis of AML cell lines. Previously, we had also described the synergistic activity of the combinations of HA-HDI with the Bcr-Abl kinase inhibitors imatinib, nilotinib, and dasatinib against cultured CML cell lines with wild-type Bcr-Abl (21, 24, 25). Although nilotinib and dasatinib inhibit the most commonly observed Bcr-Abl mutants, they are ineffective against Bcr-AblT315I, which has been referred to as the "gatekeeper" threonine at residue 315 in the Abl kinase domain (31). Recently, MK-0457 was shown to have clinical activity against CML cells with the Bcr-AblT315I mutation (17). In the present studies, we have confirmed that clinically achievable concentrations of MK-0457 not only inhibit Aurora A and B activities but also attenuate the activity of wild-type and mutant forms of Bcr-Abl, including Bcr-AblT315I. This was associated with the apoptosis of cells expressing wild-type or mutant Bcr-Abl. However, importantly, our present studies show for the first time that cotreatment with MK-0457 and vorinostat synergistically induces apoptosis of CML cell lines or BaF3 cells with wild-type or the mutant Bcr-AblE255K and Bcr-AblT315I.

The expression and activity of Aurora A and B are regulated in a cell cycle–dependent manner, with up-regulation in the G_2-M phase and rapid down-regulation after mitosis (1–3). Although not amplified, expression of Aurora A and B was easily detectable in cultured and primary AML and CML cells. Treatment with MK-0457 inhibited p-Aurora A and p-Aurora B

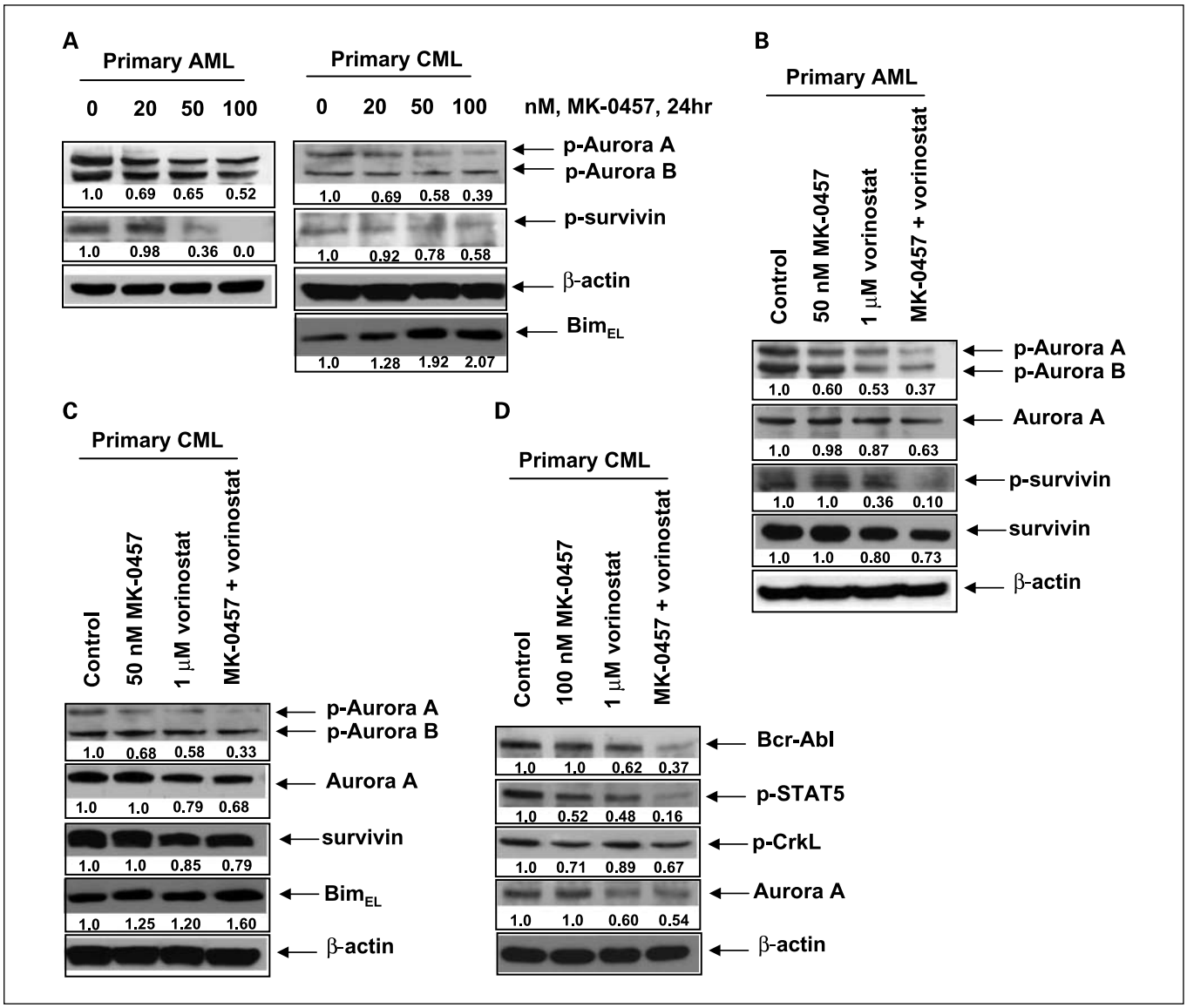

Fig. 5. The effect of MK-0457 and/or vorinostat on primary AML and CML cells. *A,* primary AML and CML cells were treated with the indicated concentrations of MK-0457 for 24 h. After this, Western blot analysis was done for p-Aurora A/B and p-survivin. The levels of β-actin in the total cell lysates served as the loading control. *B* and *C,* primary AML and CML cells were treated with the indicated concentrations of MK-0457 and/or vorinostat for 24 h. Following this, immunoblot analysis was done for p-Aurora A, Aurora A, p-survivin, and survivin. The levels of β-actin in the cell lysates served as the loading control. *D,* primary CML cells were treated with the indicated concentrations of MK-0457 and/or vorinostat for 24 h. Then, immunoblot analysis was done for Bcr-Abl, p-STAT5, p-CrkL, and Aurora A. The levels of β-actin in the cell lysates served as the loading control.

levels in the acute leukemia cells, suggesting that it inhibits the autophosphorylation activities of Aurora A and B (9). This was accompanied by decreased phosphorylation of serine 10 on histone H3 and reduced levels of p-survivin, both substrates of Aurora B (1, 3, 13). Concomitantly, treatment with MK-0457 also caused aberrant centrosome duplication, as well as induced multipolar spindle formation, G_2-M phase accumulation, decreased MPM-2 mitotic phosphoprotein staining, endoreduplication, and apoptosis of AML and CML cells (13). MK-0457 has been reported to induce endoreduplication in cells with a compromised postmitotic checkpoint, thereby allowing cells to proceed through S phase without undergoing cell division and cytokinesis (14). Cells which fail to divide accumulate greater than 8N DNA content and ultimately undergo cell death (13, 14). As previously reported, treatment with vorinostat induced Bim, a proapoptotic protein induced in leukemia cells by the forkhead family of transcription factors, which also lowers the threshold for apoptosis (32). Unlike MK-0457, vorinostat treatment depleted the protein levels of Aurora A and B in AML and CML cells. The underlying mechanism may be manifold. First, by inhibiting HDAC6, vorinostat induced hsp90 acetylation (Fig. 2A). This has been shown to inhibit the ATP-binding and chaperone function of hsp90 (23, 25), which in turn abrogates the chaperone association of hsp90 with its client proteins including Bcr-Abl, FLT-3, and c-Raf, promoting their degradation by the 26S proteasome (23, 26). HDAC inhibitors have recently been reported to deplete the association of Aurora A with hsp90, thereby promoting its degradation by the proteasome (28). This is consistent with our findings demonstrating decreased chaperone association of hsp90 with Aurora A in hsp90 immunoprecipitates and that cotreatment with bortezomib partly restores the depletion of Aurora A caused by vorinostat. Although not shown, HDAC inhibitors such as vorinostat may in part transcriptionally down-regulate Aurora A and B. Taken together, these observations may explain vorinostat-mediated down-regulation of the activity and levels of Aurora A and B.

Although the precise mechanism(s) underlying the synergistic apoptotic effects of the combination of vorinostat and MK-0457 against AML cells is not clear, several intracellular perturbations induced by the combination may explain this synergy. As compared with either agent alone, cotreatment with vorinostat plus MK-0457 induced marked inhibition of p-Aurora A and B, greater depletion of p-survivin and survivin, and more attenuation of phosphorylated serine 10 on histone H3 (data not shown) in OCI-AML3 and HL-60 cells. In contrast, as compared with treatment with vorinostat alone, cotreatment with MK-0457 and vorinostat caused similar depletion of Aurora A and B. However, cotreatment with vorinostat and MK-0457 caused more up-regulation of Bim isoforms, thus further sensitizing AML cells to the cytotoxicity of the combination. Collectively, more potent inhibition of the activities of Aurora kinases and survivin, combined with greater induction of Bim may be responsible for the superior anti-AML activity of vorinostat plus MK-0457. Similar to AML cells, as compared with treatment with vorinostat alone, cotreatment with MK-0457 and vorinostat also caused more depletion of p-survivin and phosphorylated serine 10 on histone H3 in K562 cells, but similar effects on the levels of Aurora A and Aurora B. However, combination of vorinostat and MK-0457 attenuated the activities of both Aurora and Bcr-Abl kinases, which may explain its synergistic apoptotic effects in K562 cells. In phase I/II clinical trials, MK-0457 showed significant clinical activity in patients with imatinib mesylate–resistant CML producing clinical responses in three patients (17). The T315I mutation in Bcr-Abl mediates clinical resistance to the current targeted therapeutic agents, imatinib, nilotinib, and dasatinib (31). The activity of MK-0457 against Bcr-Abl mutants in which other tyrosine kinases fail, particularly against Bcr-AblT315I, may be due to the manner in which MK-0457 binds to the Abl kinase domain. Crystal structures of MK-0457 with the Bcr-Abl kinase domain show that MK-0457 does not bind deeply to the Abl kinase domain and unlike imatinib, nilotinib, and dasatinib, this binding is not disrupted by the steric hindrance of a threonine to isoleucine substitution at residue 315 (15, 31). This attribute of MK-0457 allows it to associate with an active conformation of Bcr-Abl and inhibit the kinase activity of mutant Bcr-Abl in imatinib mesylate–resistant CML cells. In preclinical models, vorinostat has also been shown to deplete the levels of mutant forms of Bcr-Abl and exerts enhanced cytotoxic effects of dasatinib against mutant Bcr-AblE255K and Bcr-Abl T315I–containing cells (25). Therefore, consistent with these findings, our present results show that cotreatment with vorinostat and MK-0457 more effectively depletes Bcr-AblE255K and Bcr-AblT315I levels and exerts synergistic apoptotic effects against imatinib-resistant mutant Bcr-AblE255K and Bcr-Abl T315I–expressing cells.

Our findings also show the superior activity of MK-0457 plus vorinostat, as compared with treatment with either agent alone, against primary AML and imatinib-refractory CML cells. However, the effects were variable and less than additive. However, the antileukemia effects of the combination were associated with more inhibition of the activities of Aurora kinases and greater induction of Bim in AML cells. In CML cells, in addition to its inhibitory effects on Aurora kinases, the combination produced greater depletion of Bcr-Abl and its phosphorylated substrates p-STAT5, as well as more induction of Bim. Taken together, these findings are consistent with more lethal effects of the combination against primary AML and CML cells. Recent studies have highlighted that cytokinetically quiescent CML stem cells may escape the lethal effect of Bcr-Abl kinase inhibitors because they also harbor refractory Bcr-Abl mutations or possess membrane transporters of which the Bcr-Abl kinase inhibitor may be a substrate (33–35). A recent report has highlighted that hsp90 inhibitors may also have activity against Bcr-Abl expressing CML stem cells (36). Because pan-HDAC inhibitors such as vorinostat also inhibit hsp90 function, in combination with MK-0457, they may also exert cytotoxic effects against CML stem cells. Our findings also show that the combination is relatively less toxic against normal CD34+ human bone marrow progenitor cells. Taken together with previous reports, our preclinical findings presented here create a strong rationale for *in vivo* testing of the combined treatment with vorinostat and MK-0457 for AML and for CML resistant to Bcr-Abl kinase inhibitors.

Disclosure of Potential Conflicts of Interest

Coauthor Carolyn Buser is an employee of Merck & Co., Inc., and the corresponding author, Kapil Bhalla, has received a clinical and laboratory research grant from Merck & Co., Inc. All other authors have no competing financial interests.

References

1. Keen N, Taylor S. Aurora-kinase inhibitors as anticancer agents. Nat Rev Cancer 2004;4:927–36.
2. Marumoto T, Zhang D, Saya H. Aurora-A—a guardian of poles. Nat Rev Cancer 2005;5:42–50.
3. Fu J, Bian M, Jiang Q, Zhang C. Roles of Aurora kinases in mitosis and tumorigenesis. Mol Cancer Res 2007;5:1–10.
4. Fukushige S, Waldman FM, Kimura M, et al. Frequent gain of copy number on the long arm of chromosome 20 in human pancreatic adenocarcinoma. Genes Chromosomes Cancer 1997;19:161–9.
5. Nishida N, Nagasaka T, Kashiwagi K, Boland CR, Goel A. High copy amplification of the Aurora-A gene is associated with chromosomal instability phenotype in human colorectal cancers. Cancer Biol Ther 2007;6:525–33.
6. Zhou H, Kuang J, Zhong L, et al. Tumour amplified kinase STK15/BTAK induces centrosome amplification, aneuploidy and transformation. Nat Genet 1998;20:189–93.
7. Bischoff JR, Anderson L, Zhu Y, et al. A homologue of Drosophila aurora kinase is oncogenic and amplified in human colorectal cancers. EMBO J 1998;17:3052–65.
8. Schmit TL, Ahmad N. Regulation of mitosis via mitotic kinases: new opportunities for cancer management. Mol Cancer Ther 2007;6:1920–31.
9. Zhang Y, Ni J, Huang Q, Ren W, Yu L, Zhao S. Identification of the auto-inhibitory domains of Aurora-A kinase. Biochem Biophys Res Commun 2007;357:347–52.
10. Hirota T, Kunitoku N, Sasayama T, et al. Aurora-A and an interacting activator, the LIM protein Ajuba, are required for mitotic commitment in human cells. Cell 2003;114:585–98.
11. Wang X, Zhou YX, Qiao W, et al. Overexpression of aurora kinase A in mouse mammary epithelium induces genetic instability preceding mammary tumor formation. Oncogene 2006;25:7148–58.
12. Carvajal RD, Tse A, Schwartz GK. Aurora kinases: new targets for cancer therapy. Clin Cancer Res 2006;12:6869–75.
13. Harrington EA, Bebbington D, Moore J, et al. VX-680, a potent and selective small-molecule inhibitor of the Aurora kinases, suppresses tumor growth *in vivo*. Nat Med 2004;10:262–7.
14. Gizatullin F, Yao Y, Kung V, Harding MW, Loda M, Shapiro GI. The Aurora kinase inhibitor VX-680 induces endoreduplication and apoptosis preferentially in cells with compromised p53-dependent post mitotic checkpoint function. Cancer Res 2006;66:7668–77.
15. Young MA, Shah NP, Chao LH, et al. Structure of the kinase domain of an imatinib-resistant Abl mutant in complex with the Aurora kinase inhibitor VX-680. Cancer Res 2006;66:1007–14.
16. Cheetham GM, Charlton PA, Golec JM, Pollard JR. Structural basis for potent inhibition of the Aurora kinases and a T315I multi-drug resistant mutant form of Abl kinase by VX-680. Cancer Lett 2007;251:323–9.
17. Giles FJ, Cortes J, Jones D, Bergstrom D, Kantarjian H, Freedman SJ. MK-0457, a novel kinase inhibitor, is active in patients with chronic myeloid leukemia or acute lymphocytic leukemia with the T315I BCR-ABL mutation. Blood 2007;109:500–2.
18. Dokmanovic M, Clarke C, Marks PA. Histone deacetylase inhibitors: overview and perspectives. Mol Cancer Res 2007;5:981–9.
19. Minucci S, Pelicci PG. Histone deacetylase inhibitors and the promise of epigenetic (and more) treatments for cancer. Nat Rev Cancer 2006;6:38–51.
20. Glozak MA, Seto E. Histone deacetylases and cancer. Oncogene 2007;26:5420–32.
21. Nimmanapali R, Fuino L, Bali P, et al. Histone deacetylase inhibitor LAQ824 both lowers expression and promotes proteasomal degradation of Bcr-Abl and induces apoptosis of imatinib mesylate-sensitive or -refractory chronic myelogenous leukemia-blast crisis cells. Cancer Res 2003;63:5126–35.
22. Guo F, Sigua C, Tao J, et al. Cotreatment with histone deacetylase inhibitor LAQ824 enhances Apo-2L/tumor necrosis factor-related apoptosis inducing ligand-induced death inducing signaling complex activity and apoptosis of human acute leukemia cells. Cancer Res 2004;64:2580–9.
23. Bali P, Pranpat M, Bradner J, et al. Inhibition of histone deacetylase 6 acetylates and disrupts the chaperone function of heat shock protein 90: a novel basis for antileukemia activity of histone deacetylase inhibitors. J Biol Chem 2005;280:26729–34.
24. Fiskus W, Pranpat M, Bali P, et al. Combined effects of novel tyrosine kinase inhibitor AMN107 and histone deacetylase inhibitor LBH589 against Bcr-Abl expressing human leukemia cells. Blood 2006;108:645–52.
25. Fiskus W, Pranpat M, Balasis M, et al. Cotreatment with vorinostat (suberoylanilide hydroxamic acid) enhances activity of dasatinib (BMS-354825) against imatinib mesylate-sensitive or imatinib mesylate-resistant chronic myelogenous leukemia cells. Clin Cancer Res 2006;12:5869–78.
26. Bali P, George P, Cohen P, et al. Superior activity of the combination of histone deacetylase inhibitor LAQ824 and the FLT-3 kinase inhibitor PKC412 against human acute myelogenous leukemia cells with mutant FLT-3. Clin Cancer Res 2004;10:4991–7.
27. Lange BM, Rebollo E, Herold A, González C. Cdc37 is essential for chromosome segregation and cytokinesis in higher eukaryotes. EMBO J 2002;21:5364–74.
28. Park JH, Jong HS, Kim SG, et al. Inhibitors of histone deacetylases induce tumor-selective cytotoxicity through modulating Aurora-A kinase. J Mol Med 2008;86:117–28.
29. Yang J, Ikezoe T, Nishioka C, et al. AZD1152, a novel and selective aurora B kinase inhibitor, induces growth arrest, apoptosis, and sensitization for tubulin depolymerizing agent or topoisomerase II inhibitor in human acute leukemia cells *in vitro* and *in vivo*. Blood 2007;110:2034–40.
30. Chou TC, Talalay P. Quantitative analysis of dose-effect relationships: the combined effects of multiple drugs or enzyme inhibitors. Adv Enzyme Regul 1984;22:27–55.
31. Weisberg E, Manley PW, Cowan-Jacob S, et al. Second generation inhibitors of BCR-ABL for the treatment of imatinib-resistant chronic myeloid leukemia. Nat Rev Cancer 2007;7:345–58.
32. Essafi A, Fernandez de Mattos S, Hassen YAM, et al. Direct transcriptional regulation of Bim by FoxO3a mediates STI571-induced apoptosis in Bcr-Abl-expressing cells. Oncogene 2005;24:2317–29.
33. Jiang X, Saw KM, Eaves A, Eaves C. Instability of BCR-ABL gene in primary and cultured chronic myeloid leukemia stem cells. J Natl Cancer Inst 2007;99:680–93.
34. Deininger MW. Optimizing therapy of chronic myeloid leukemia. Exp Hematol 2007;35:144–54.
35. Chu S, Xu H, Shah NP, et al. Detection of BCR-ABL kinase mutations in CD34+ cells from chronic myelogenous leukemia patients in complete cytogenetic remission on imatinib mesylate treatment. Blood 2005;105:2093–8.
36. Peng C, Brain J, Hu Y, et al. Inhibition of heat shock protein 90 prolongs survival of mice with BCR-ABL-T315I-induced leukemia and suppresses leukemic stem cells. Blood 2007;110:678–85.